Revista de Metalurgia
October-December 2023, 59 (4), e249
ISSN-L: 0034-8570
https://doi.org/10.3989/revmetalm.249

Wear performance of GGG60 ductile iron rollers coated with WC-Co by electro spark deposition

Mustafa Buğday[a,*], Mehmet Karalı[b], Şükrü Talaş[c]

[a] Department of Mechanical Engineering, Karabuk University, Karabuk 78050, Turkey

[b] Department of Mechatronics Engineering, Necmettin Erbakan University, Konya 42140, Turkey

[c] Department of Metallurgical and Materials Engineering, Afyon Kocatepe University, Afyonkarahisar, 03200, Turkey

(*Corresponding author: mustafabugday@karabuk.edu.tr)

Submitted: 24 April 2023; Accepted: 29 November 2023; Available On-line: 3 January 2023

ABSTRACT: Nodular cast irons are used in many industrial applications such as machine frames and body, rollers and engine blocks due to their higher strengths and ductility with good machinability comparable to grey cast irons. In this study, the outer surface of nodular cast irons (GGG-60) was coated with WC/Co using electro spark deposition (ESD). The aim of the study is to improve both the surface quality and wear behaviour with the coatings formed on the surface of the plastic deformation rollers, whose wear resistance decreases over the time due to high stress working conditions. Heat treatment at 950 ºC for 2 h was applied to the GGG60 specimen rollers and half of the rollers were uncoated and the other half was coated with WC-Co electrodes. The wear behaviour of the heat treated and coated surfaces was measured by ball-on-disc wear method using Al_2O_3 ball bearing with a diameter of 6 mm for a sliding distance of 250 m at a sliding rate of 6.5 $m \cdot s^{-1}$ under a dry condition, and using a load of 40 N. WC/Co coatings were successfully applied to rollers. In the SEM/EDS images, the presence of W, Fe, C, Co and Al elements in the coated part of the rollers and Fe, C and Al elements in the uncoated region were detected. It was concluded that Coating and heat treatment increased the wear resistance by nearly 5 times and decreased the friction coefficient by 2.13 times.

KEYWORDS: Coating; Cobalt; Electro spark deposition; Rolling; Tungsten carbide; Wear

Citation/Citar como: Buğday, M.; Karalı, M.; Talaş, S. (2023). "Wear performance of GGG60 ductile iron rollers coated with WC-Co by electro spark deposition". *Rev. Metal.* 59(4): e249. https://doi.org/10.3989/revmetalm.249

RESUMEN: *Comportamiento frente al desgaste de rodillos de fundición dúctil GGG60 recubiertos con WC-Co mediante electrodeposición por chispa***.** Las fundiciones nodulares se utilizan en muchas aplicaciones industriales, como bastidores y carrocerías de máquinas, rodillos y bloques de motor, debido a su mayor resistencia y ductilidad con una buena maquinabilidad comparable a la de las fundiciones grises. En este estudio, la superficie exterior de las fundiciones nodulares (GGG-60) se recubrió con WC/Co mediante electrodeposición por chispa (ESD). El objetivo del estudio es mejorar tanto la calidad superficial como el comportamiento frente al desgaste con los recubrimientos formados sobre la superficie de los rodillos deformados plásticamente, cuya resistencia al desgaste disminuye con el tiempo debido a las condiciones de trabajo de alto esfuerzo. Se aplicó un tratamiento térmico a 950 ºC durante 2 h a los rodillos de GGG60 y la mitad de los rodillos se dejaron

sin recubrir y la otra mitad se recubrió con electrodos de WC-Co. El comportamiento al desgaste de las superficies tratadas térmicamente y recubiertas se midió mediante el método de desgaste bola sobre disco utilizando bolas de Al_2O_3 con un diámetro de 6 mm para una distancia de deslizamiento de 250 m a una velocidad de deslizamiento de 6,5 $m \cdot s^{-1}$ en condiciones secas y utilizando una carga de 40 N. Los recubrimientos de WC/Co se aplicaron con éxito a los rodillos. En las imágenes SEM/EDS se detectó la presencia de elementos de W, Fe, C, Co y Al en la parte recubierta de los rodillos y de elementos de Fe, C y Al en la región no recubierta. Se concluyó que el recubrimiento y el tratamiento térmico aumentaron la resistencia al desgaste en casi 5 veces y disminuyeron el coeficiente de fricción en 2,13 veces.

PALABRAS CLAVE: Carburo de tungsteno; Cobalto; Desgaste; Electrodeposición por chispa; Laminado; Recubrimiento

ORCID ID: Mustafa Buğday (https://orcid.org/0000-0003-4413-509X); Mehmet Karalı (https://orcid.org/0000-0002-2380-0575); Şükrü Talaş (https://orcid.org/0000-0002-4721-0844)

1. INTRODUCTION

Hot rolling of metals is one of the most effective plastics forming methods used in the mass production of different geometric shapes for which the metal stock is passed through pairs of rolls. The metal plates are rolled to reduce the thickness and are given specific shapes for desired application. In different mechanical conditions, rolls are exposed to compression, shear, bending, or torsional stresses depending on various operating conditions (Xu *et al.*, 2017; Cheng *et al.*, 2017). Such stresses during the rolling operation increase the wear on the roller and affect the surface quality of the final product. It is possible to prevent such situations that limit the life of the roller with the improvements made on the roller (Tieu *et al.*, 2011; Phan *et al.*, 2017). Due to its features such as high wear resistance, tensile strength, oxidation resistance, ductility, rolling mills are made of spheroidal or nodular graphite cast iron (also called Ductile Iron or GGG in the literature) in industry (Yang *et al.*, 2013; Faisal *et al.*, 2019). However, different operating conditions significantly affect the wear performance of the rollers produced from this type of material. Although it is recommended in the literature that the wear performance can be improved by methods such as alloying addition, this causes a decrease in the ductility and formability of the roller material as a result of changes in the internal structure of the material (Alhussein *et al.*, 2014; Kim *et al.*, 2008). Recently, it has become possible to prevent such problems with various coating technologies (Luo *et al.*, 2015; Méndez-Medrano *et al.*, 2018; Jiang *et al.*, 2018; Rezende *et al.*, 2019; El Azhari *et al.*, 2020; Yuan *et al.*, 2021; Ling *et al.*, 2022).

ESD coating is one of the few methods that can be performed at room temperature (Chen and Zhou, 2006; Burkov and Pyachin, 2014). Since the coating layers are bonded to the substrate by alloying, it is possible to obtain fine-grained, homogeneous and thicker coatings with the ESD technique (Burkov and Pyachin, 2014; Kayalı and Talas, 2021). With this coating method, a coating layer consisting of most metal, alloy or composition can be deposited on the surface of the substrate without extensive preparation (Ruijun *et al.*, 2005; Aghajani *et al.*, 2020; Kayalı and Talas, 2021). Since the devices required for ESD technique are easy to carry and operate, they can be used in various industrial applications (Ebrahimnia *et al.*, 2014; Rukanskis, 2019). While the presence of Tungsten and Cobalt in the coating increases the wear resistance, Nickel and Molybten negatively affect the tribological properties of the coatings. In recent years, coatings in W-C-Co combination have a positive effect on wear and surface hardness values (Moura e Silva *et al.*, 2006; Vernhes *et al.*, 2013).

In this study, the wear behavior of the samples coated with WC/Co with the ESD technique was comparatively investigated. The roller used in the experimental environment was coated with WC/Co. The changes in the surface after the rolling process were investigated by SEM/EDS. Coating a rolling mill used in an experimental environment and examining it experimentally is important in terms of the study's contribution to the literature.

2. MATERIALS AND METHODS

2.1. Material and ESD coating

In this study, the wear behaviour of GGG 60 spheroidal graphite cast irons coated with WC/Co prepared in Ø20×5 mm dimensions were investigated. Then, an Ø60×70 mm rolling roll was coated with a WC/Co electrode. Images of coated cylinders are shown in Fig. 8. The changes in the roll surface as a result of the rolling process were examined. The chemical composition of the substrate material is shown in Table 1. Heat treatment was applied to improve the wear behaviour of GGG60 cast iron with low surface hardness. In the heat treatment, the samples were austenitized at 950 °C for 2 h, then, austempered at 250 °C for 2 h (Zhang *et al.*, 2014).

Table 1. Chemical Compositions of the Test Materials, wt.%, with iron to balance

GGG 60	C	Mn	P	Si	Cr	Cu
% wt	3.56	0.13	0.03	2.21	0.35	0.73

During the coating process, the substrate GGG60 roller was placed in a slot on the coating machine whose rotation speed can be adjusted. The coating process was carried out at electrode rotation speed of 230 rpm, coating voltage of 132 V and coating frequen-

cy of 1230 Hz. Argon gas was used during the process to reduce surface roughness and coating defects. The spark formation during ESD coating was achieved by gently touching the vibrating electrode applicator to the substrate material. Following each coating, ESD coated surface was cleaned using 1000G sandpaper before the next coating process.

2.2. Wear test

The tribological performances of the coatings were determined by the wear test. Wear tests (in ASTM G-77 standards) were performed with a 6 mm diameter Al_2O_3 ball on the Tribometer T10/20 (UTS) device (Fig. 1). During the wear test, samples with dimensions of Ø20×5 mm were used. The experiments were carried out in dry conditions and at room temperature, under a load of 40 N, at a sliding speed of 6.5 $m \cdot s^{-1}$, at a rotational speed of 240 rpm and at a distance of 250 m. After the wear test, the wear tracks on the surface were analyzed using Mitutoyo brand roughness tester. Friction coefficients and specific wear rates (SWR) were obtained with respect to the effect of heat treatment and coating.

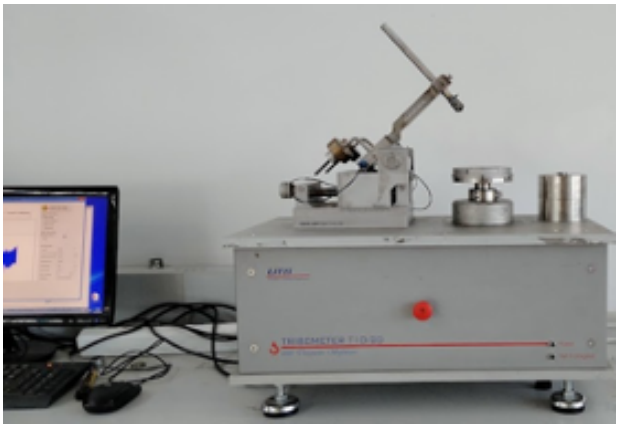

Figure 1. Tribometer T10/20 (UTS).

2.3. Hardness test

The cast samples were first sanded so that the surface hardness values could be read more easily. A load of 200 g was applied on the samples for 10 s. Emcotest – Durascan G5 Brand micro hardness measuring device was used during the experiment.

2.4. Rolling process

The rolling process was carried out on two different bars (St 37 and Al 6035) with the same dimensions (12x37.5x500 mm). Rolling forces were set as 20 kN for St 37 and 5 kN for Al6035 alloy in order to achieve similar amount of deformation ratio in strips with different surface hardness and bulk modulus values. The rolling process was carried out at a speed of 1 $m \cdot min^{-1}$. After the rolling process, sections were taken from various parts of the coated roller. Scanning electron microscopy was used to image the worn surface on both coated and uncoated surfaces. A field emission scanning electron microscope (SEM, Hitachi – SU 1510) was used to analyze the fracture morphology and defect densities in the coatings. Figure 2 shows the device used during the rolling test.

Figure 2. Rolling device.

3. RESULTS AND DISCUSSION

3.1. Wear test

The GGG60 ductile iron specimens were heat treated by fully austenitizing followed by austempering by which specimen internal stresses were drastically removed. In order to evaluate the wear characteristics of the coated and uncoated ductile irons were used as a counterface disks.

The changes in the friction coefficient and SWRs of all specimens in dry conditions are given in Table 3 and Fig. 3. It can be seen that the lowest coefficient of friction occurs in the heat-treated and coated sample, and the highest coefficient of friction occurs on the substrate that is non heat treated. SWR values were calculated from the surface roughness data measured with a 2D profilometer from the wear zone. The friction coefficients of the heat-treated coated sample and non heat treated and coated specimens are almost similar to each other, i.e. 0.32 and 0.39, while the friction coefficients of the heat treated and non heat treated uncoated specimens are also higher in values i.e. 0.68 and 0.51 compared to uncoated specimens. There is an exception of a sudden drop in COF value in non heat treated and non coated specimen at around 160 m of wear experiments, which may be a result of excessive wear of metallic layer and increased ratio of graphite on the surface leading to reduced COF. It is interesting that sudden increase following the drop

Table 2. Specific Wear Rate (SWR) and Coefficients of Friction values of GGG60 specimens

Abrasive Ball Type	Al_2O_3	
Materials	Coefficient of Friction, μ	S. Wear rate x 10^{-6}, mm^3/Nm
No Heat Treatment + No Coating	0.68	169.56
Heat Treated + No Coating	0.51	97.34
No Heat Treatment + Coated with WC/Co	0.39	69.08
Heat Treated + Coated with WC/Co	0.32	33.85

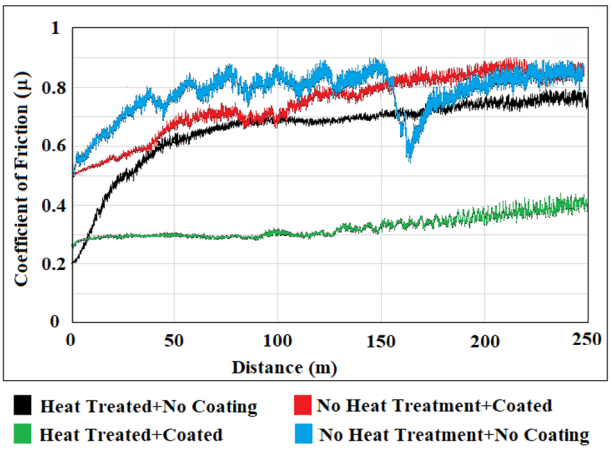

Figure 3. Coefficient of friction values with respect to the wear distance (trend line of averages of measurements).

region suggests that graphite appears to have worn off quickly and a metallic layer is formed with a high COF value. Similar COF observations are available for non heat treated ductile cast iron, being 0.54 in steady state region of COF vs. sliding distance diagram (Pagano *et al.*, 2016), which is very close to the value observed in this study. The ESD coating of GGG60 surfaces with WC+Co electrode significantly reduces the SWR but heat treatment process does not decrease it as much as WC+Co coating. SWRs follow the trend in coefficient of frictions, that is, the non heat treated specimen produced a specific wear rate of $169.56x10^{-6}$ mm^3/Nm, which is relatively high compared to $33.85x10^{-6}$ mm^3/Nm, which is obtained from heat treated and coated surface. Heat treatment and coating processes increased the wear performance 5 times more than the lowest coefficient of friction, i.e. $33.85x10^{-6}$ mm^3/Nm.

SEM/EDS images of worn surfaces after wear testing are given in Figs. 4-7. Metallic residues from delamination of the substrate due to fretting or from the action of the abrasive that gets into between the abrasive ball and the substrate, causing increased surface wear (Kayalı and Talas, 2019; Burkov and Krutikova, 2020). Repeated loads result in extensive loss of material in the form of pitting in most metallic systems, here, the non-heat treated sample produced similar form of wear with the highest wear rate. Spheroidal or nodular formation in the cast iron is believed to be partly responsible for this wear mode is it creates highly stressed zones which are easily removed during the action of ball movement on the surface. Graphite nodules are naturally in nodular formation and not strongly attached to the matrix, when it is close to the surface, graphite nodules may act like a stress raiser as the wear load is applied and passing directly on them.

Figures 4 and 5 show coated surfaces of heat treated and non-heat treated substrate GGG60 roller and cross-sectional microstructure just below the surface of GGG60 before and after heat treatment process. Non heat treated surface contains pitting appearance (Fig. 4 (a-b)) whereas heat treated surface is lacking such formation (Fig. 5 (a-b)). Optical images of surfaces (Fig. 4c and Fig. 5c) show that the surface of non-heat treated GGG60 contains more nodular structures closer to the surface while heat treated surface of GGG60 contains a decarburized region of more than 100 μm thick. This decarburised region has less graphite and

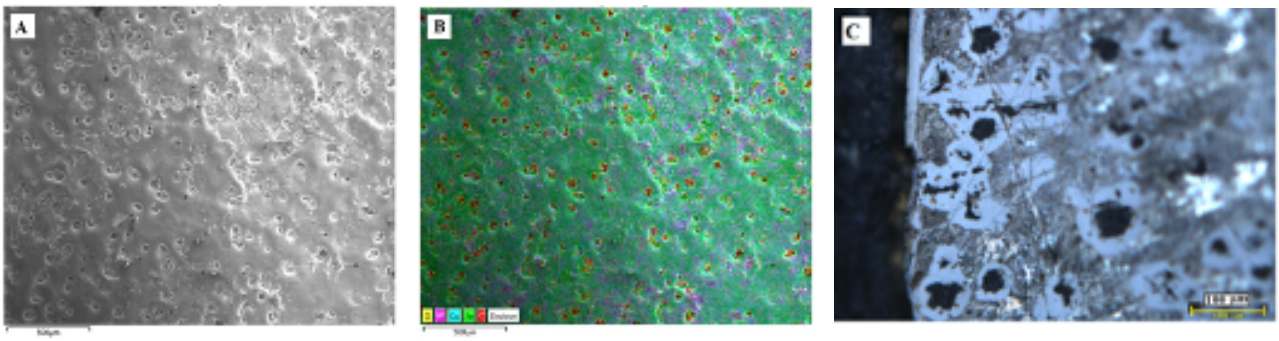

Figure 4. Non heat treated and WC-Co coated GGG60 specimen surface a) SEM image and b) Elemental mapping image and c) optical image of microstructure just below the surface of GGG60 before heat treatment.

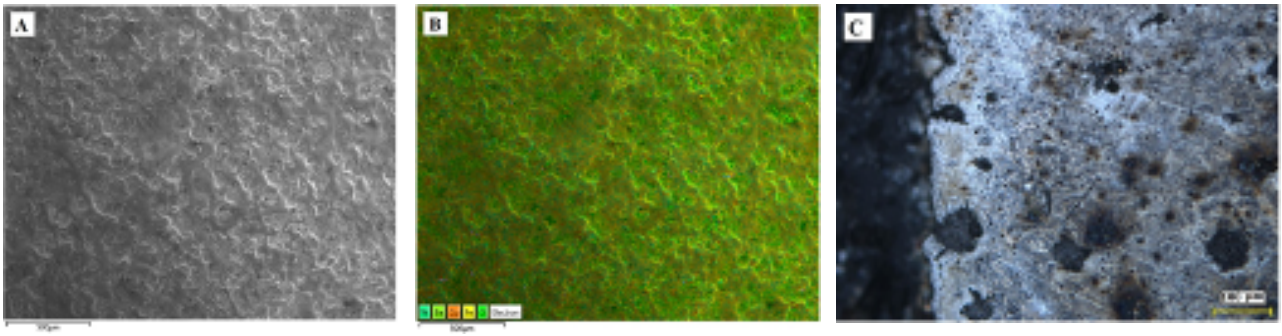

Figure 5. Heat treated and WC-Co coated GGG60 specimen surface a) SEM image and b) Elemental mapping image and c) optical image of microstructure just below the surface of GGG60 after heat treatment.

more ferritic microstructure which is apparent due to its light metallic colour. Heat treated surface was in contact with air and some of graphite nodules and C in matrix are believed to have generated CO during the heat treatment, leading to the formation of CO_2 with two step reactions (Moormann, 2011) and hence the number and/or size of the graphite nodules on the surface is likely to be reduced significantly. It is also possible that decarburization helps to produce a good metallurgical bonding by non-wetting of graphite due its high surface tension which leads to pitted appearance. The substrate iron matrix with less graphite and carbon in matrix of cementite/bainitic/martensitic would also help produce a good metallurgical bonding during the micro welding action, too. The high carbon content presents difficulty in weldability of steels in general (Cárcel Carrasco *et al.*, 2022). The melting point of the alloy of substrate and electrode material is likely to rise above 1600 ºC, on the other hand, graphite sublimates at 3550 ºC, which shows that graphite is significantly heat-resistant enough to withstand the temperature of molten metal which remains as alloying liquid very briefly during the coating process.

Figure 6 and Fig. 7 show SEM images and EDX mapping of heat treated and non-heat treated and coated GGG60 surfaces, respectively. It is easily observed that the most of the delamination are from the regions where graphite nodules are present near the surface. Graphite nodules can behave as stress raisers or an initiation point for fatigue wear. A flake formation is very obvious from the surface, which indicates that crack formation is very close to surface. In addition to high surface hardness of the coating, oxidative wear is thought to occur with the presence of oxide layers on

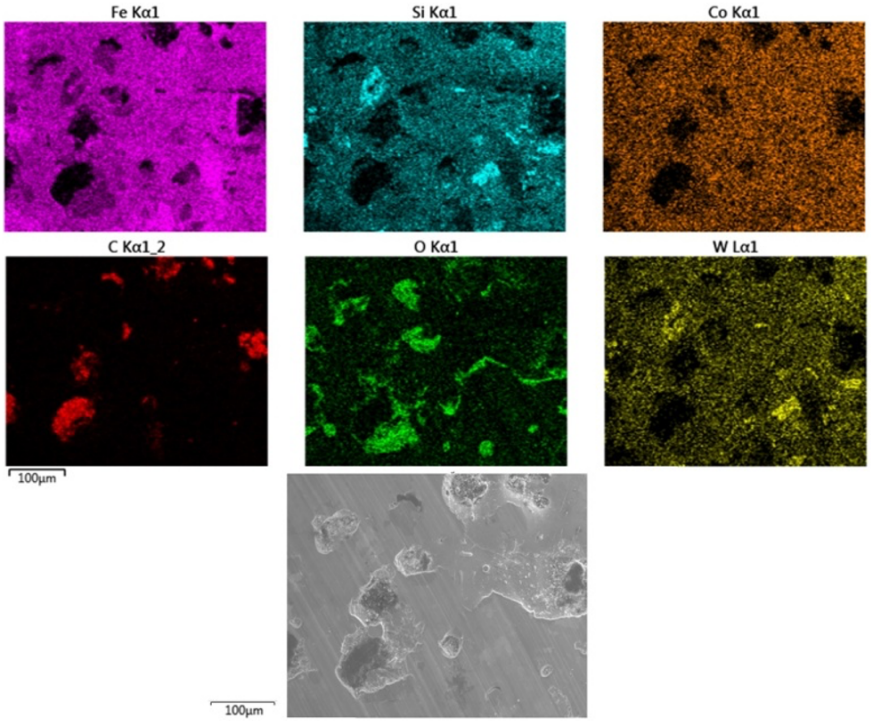

Figure 6. Worn surface of non heat treated and WC-Co coated GGG60 specimen.

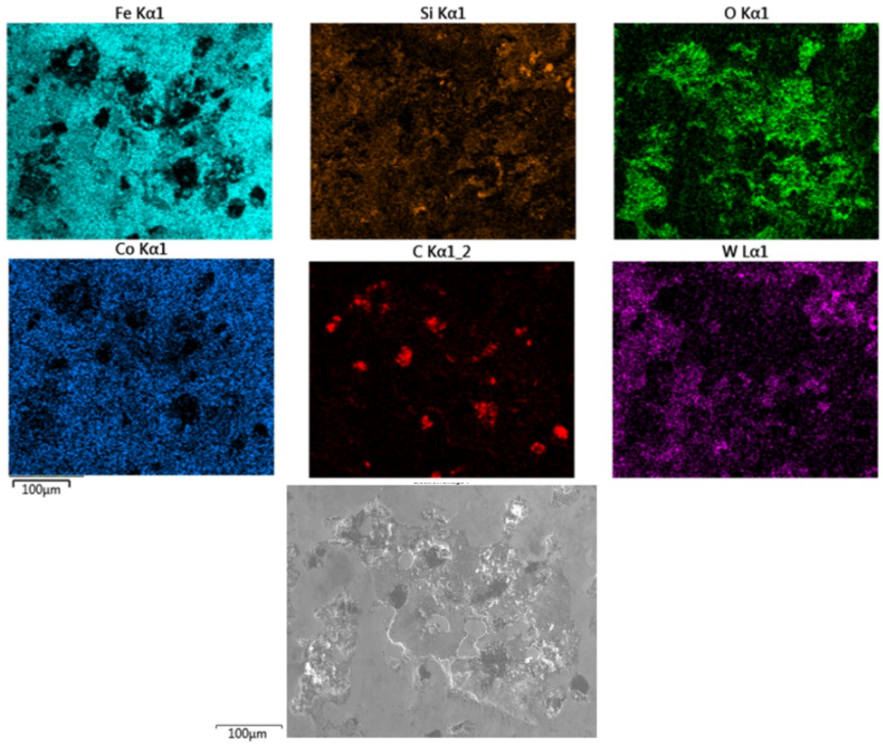

Figure 7. Worn surface of heat treated and WC-Co coated GGG60 specimen.

the heat-treated coated sample surface, generating the lowest wear rate. As seen in elemental mapping image in Fig. 6 that oxygen is mostly located around the defects where there could be high amount of heat is generated during the course of friction and oxidation reactions would take place as soon as fresh metal surface emerges. As in Fig. 6 and Fig. 7, graphite nodules are remarkably bare and there are no elemental readings on such locations as it is not wetted by the molten metal and reaction product is not present as it may have been swept away by the action of rotation of GGG60 roller and/or coating electrode during ESD coating process.

Similar observations are made with heat treated and coated GGG60 specimens as given in Fig. 7. There is remarkable difference in pattern of defects such that defects are larger and there is more oxidative wear on the surface and the sizes of the graphite nodules appear to be less than those of non-heat treated surface given in Fig. 6. There are regions where fatigue loading and eventual delamination are very evident, especially in the middle of the image where W elements are not observed. As W is mostly present in the coating, the hard coating layer is presumably delaminate due to fretting wear which is followed by the oxidative wear as seen in O element imaging in Fig. 7. Co elemental distribution is also interesting to note that Co is present in most of the matrix as opposed to W, as the solubility of Co in Fe is relatively high compared to W in Fe (Zhu *et al.*, 2001; Chang and Chen, 2014); which in excess of C (graphite) produces WC+C or $W_2C(\alpha)$+WC phases. In the absence of excessive C, the formation of W_2C is encouraged and the formation of W is also possible following the ESD coating (Whang *et al.*, 2009; Korkmaz, 2015). Similar to this observation with C, there is also matching zones between W and Si in both elemental mapping images in Figs. 6 and 7. In Figs. 6 and 7, Si locations are intensely bright as with W locations in same position where W possibly reacts with Si to form WSi_2 or W_5Si_3 compound during the coating (Guo *et al.*, 2009). However, in Fig. 6, the intensity of Si and W points are less compared to Fig. 6, which indicate that the heat treatment may have removed some amount of Si during decarburization in heat treatment.

3.2. Hardness test

WC in the coatings increases microhardness of the matrix. The presence of W_2C phases and W elements in the coatings significantly improves the hardness and wear resistance of the coatings. When WC ceramic material is used together with elements such as Ni and Co, it can be easier to adhere to the substrate sample. Here, Ni and Co elements are used as binding materials. The use of bonding elements makes it difficult for cracks to form and spread within the coating and increases the hardness values of the coatings (Burkov and Pyachin, 2014; Ebrahimnia *et al.*, 2014; Rukanskis, 2019; Kayalı and Talas, 2021).

The average of the data read from at least five places during the test was taken. In the first case, the average surface hardness value of the GGG 60 sample was calculated as 270 ± 5.6 $HV_{0.2}$. As a result of

heat treatment, the average surface hardness value was measured as 540 ± 9 $HV_{0.2}$. In the ongoing study, un-heat-treated and treated samples were coated with WC / 12% Co electrode material. As a result of coating, the average surface hardness value was measured as 1107 ± 8 $HV_{0.2}$ in the coated sample without heat treatment and 1330 ± 12.5 $HV_{0.2}$ in the coated sample with heat treatment. This value overlaps with other studies in the literature. Table 3 gives the surface hardness values of the samples. According to Table 3, while heat treatment increased the surface hardness value of the samples by 2 times, WC-Co coating applied with ESD increased the surface hardness value of the samples by 5 times.

Table 3. Surface Hardness Test Results

Materials	Hardness Value $HV_{0.2}$
No Heat Treatment + No Coating	270 ± 5.6
Heat Treated + No Coating	540 ± 9
No Heat Treatment + Coated with WC/Co	1107 ± 8
Heat Treated + Coated with WC/Co	1330 ± 12.5

3.3. Rolling process

St 37 and Al 6035 series strips were rolled under a rolling force of 20 kN and 5 kN, respectively. It was observed that fracture occurred along the keyway after 100 m of rolling of the St 37 strips. The designed roll showed poor performance under high rolling forces. It is considered possible to optimize such errors with better designs. However, the rolling process of Al 6035 series bar was successfully carried out and following the rolling process, the presence of Al base metal was detected in the middle part of the roller. In Fig. 8, imag-

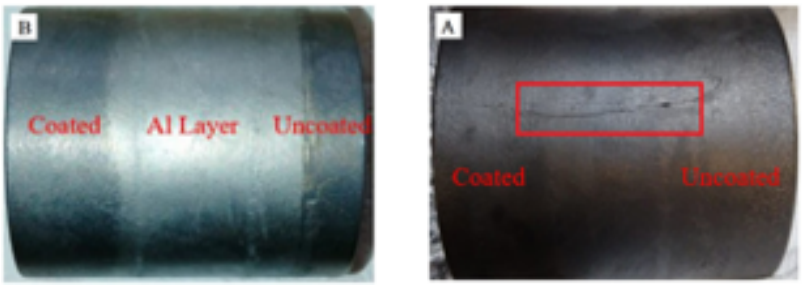

Figure 8. Images of roller surfaces after rolling with a) St 37 and b) Al 6035.

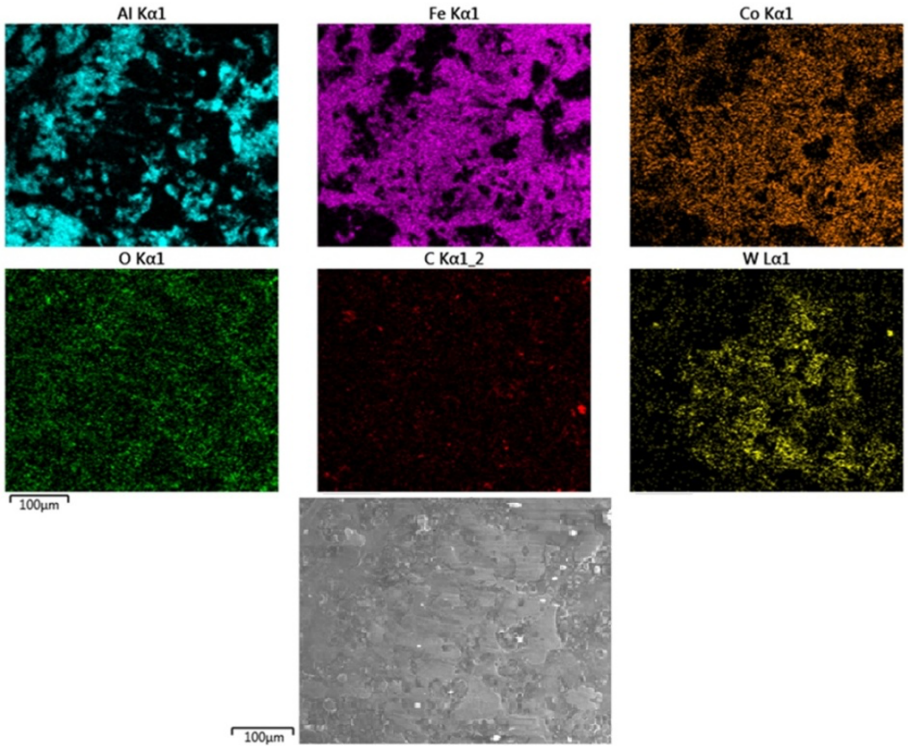

Figure 9. Surface images after rolling from WC-Co coated surface a) SEM b) EDS.

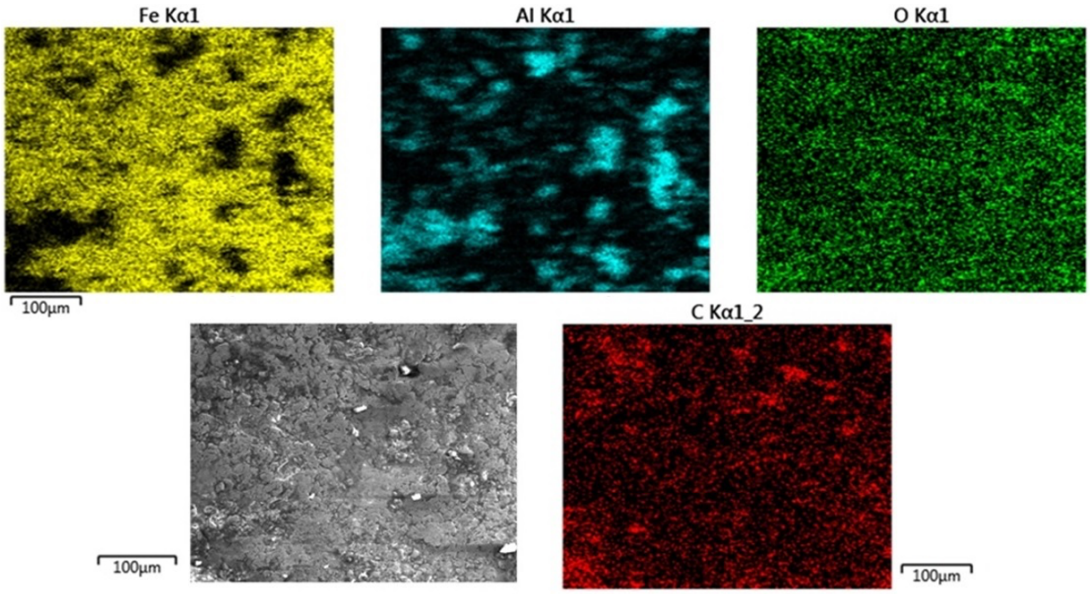

Figure 10. Surface images after rolling from uncoated surface a) SEM b) EDS.

es of the roller after the rolling process with St 37 (Fig. 7a) and Al 6035 plates (Fig. 7b) are given.

After the rolling process of Al alloy plates, SEM/EDS images were obtained from WC-Co coated and uncoated parts of the roller surfaces. The presence of coating elements were determined using EDX analysis, although, the aluminum layer hindered the coating elements (W, C, Co) from being detected in the sections where aluminum is rolled. Aluminum, being a softer material than the coating, did not cause any wear on the roller surface, in fact, produced an extra coating on the surface of the roller and WC/Co layer. The transfer of Al onto the surface of GGG60 substrate is expected due to the application of high rolling forces. The SEM/EDX images given in Fig. 9 and Fig. 10 supports this conclusion. After rolling of aluminum strips, the surface roughness decreased from 1.094 µm to 0.557 µm. It is thought that the aluminum layer formed on the surface fills the void structures between the coating asperities and therefore the final surface roughness value is consequently lower following the rolling operation with Al6035 alloy. As it can be seen in Fig. 9 and Fig. 10 EDX mapping images that Aluminum presence with Oxygen is more obvious.

4. CONCLUSIONS

In this study, the effect of heat treatment and WC+Co coating by ESD process on wear behaviour of GGG60 was investigated. ESD coated GGG60 roller was then experimentally tested using Al6035 Al alloy. After the rolling process, various changes on the surface were observed. Major outcomes of this study are given below.

- Wear resistance of GGG 60 ductile cast iron is increased with WC/Co coating. The lowest wear rate was obtained in the heat-treated coated sample (33.85×10^{-6} mm^3/Nm), and the highest wear rate was obtained in the substrate sample (169.56×10^{-6} mm^3/Nm). With WC/Co coating, the wear resistance of cast iron has been increased by nearly 5 times.
- The roller used in the experimental study was coated with a WC/Co electrode, which showed a strong metallurgical attachment to the surface when GGG60 heat treated due to decarburisation.
- Following the rolling with an Al 6035 bar, the presence of an Al layer on the surface of the roller was detected but there was no detection of Aluminium on the worn surfaces.
- The presence of W, Co and C elements was detected on the surface as a result of SEM/EDS analysis which can be considered as proof that rolling does not damage the coatings.
- Al layer filled the gaps between the coating elements (W, Co, C), causing the surface roughness value to decrease. As a result, the surface roughness value decreased from 1.094 µm to 0.557 µm.

ACKNOWLEDGMENTS

This study was supported by the project number of 221419003 obtained from Scientific Support Unit of Necmettin Erbakan University.

REFERENCES

Aghajani, H., Hadavand, E., Peighambardoust, N.S., Khameneh-asl, S. (2020). Electro spark deposition of WC–TiC–Co–Ni cermet coatings on St52 steel. *Surfaces and Interfaces* 18, 100392. https://doi.org/10.1016/j.surfin.2019.100392.

Alhussein, A., Risbet, M., Bastien, A., Chobaut, J.P., Balloy, D., Favergeon, J. (2014). Influence of silicon and addition

elements on the mechanical behavior of ferritic ductile cast iron. *Mater. Sci. Eng. A* 605, 222-228. https://doi.org/10.1016/j.msea.2014.03.057.

Burkov, A.A., Pyachin, S.A. (2014). Investigation of WC-Co electrospark coatings with various carbon contents. *J. Mater. Eng. Perform.* 23, 2034-2042. https://doi.org/10.1007/s11665-014-0974-z.

Burkov, A.A., Krutikova, V.O. (2020). Deposition of Amorphous Hardening Coatings by Electrospark Treatment in a Mixture of Crystalline Granules. *Russ. J. Non-Ferrous Met.* 61, 132-141. https://doi.org/10.3103/S1067821220010022.

Cárcel Carrasco, J., Salas Vicente, F., Martínez Corral, A., Pascual Guillamón, M. (2022). Weldability of ductile cast iron using AISI-316L stainless steel ER rod. *Rev. Metal.* 58 (3), e224. https://doi.org/10.3989/revmetalm.224.

Chang, S.H., Chen, S.L. (2014). Characterization and properties of sintered WC–Co and WC–Ni–Fe hard metal alloys. *J. Alloys Compd.* 585, 407-413. https://doi.org/10.1016/j.jallcom.2013.09.188.

Chen, Z., Zhou, Y. (2006). Surface modification of resistance welding electrode by electro-spark deposited composite coatings: Part I. Coating characterization. *Surf. Coat. Tech.* 201 (3-4), 1503-1510. https://doi.org/10.1016/j.surfcoat.2006.02.015.

Cheng, X., Jiang, Z., Wei, D., Hao, L., Wu, H., Xia, W., Zang, X., Luo, S., Jiang, L. (2017). Effects of surface preparation on tribological behaviour of a ferritic stainless steel in hot rolling. *Wear* 376-377, 1804-1813. https://doi.org/10.1016/j.wear.2017.01.106.

Ebrahimnia, M., Ghaini, F. M., Xie, Y. J., Shahverdi, H. (2014). Microstructural characteristics of the built-up layer of a precipitation hardened nickel based superalloy by electrospark deposition. *Surf. Coat. Tech.* 258, 515-523. https://doi.org/10.1016/j.surfcoat.2014.08.045.

El Azhari, I., García, J., Zamanzade, M., Soldera, F., Pauly, C., Motz, C., Llanes, L., Mücklich, F. (2020). Micromechanical investigations of CVD coated WC-Co cemented carbide by micropillar compression. *Mater. Des.* 186, 108283. https://doi.org/10.1016/j.matdes.2019.108283.

Faisal, M., El-Shenawy, E., Taha, M.A. (2019). Effect of Deformation Parameters on Microstructural Evolution of GGG 40 Spheroidal Graphite Cast Iron Alloy. *Mater. Sci. Appl.* 10 (06), 433. https://doi.org/10.4236/msa.2019.106032.

Guo, Z., Yuan, W., Sun, Y., Cai, Z., Zyu, Q. (2009). Thermodynamic assessment of the Si-Ta and Si-W systems. *J. Phase Equilibria Diffus.* 30, 564–570. https://doi.org/10.1007/s11669-009-9579-x.

Jiang, W., Shen, L., Qiu, M., Wang, X., Fan, M., Tian, Z. (2018). Preparation of Ni-SiC composite coatings by magnetic field-enhanced jet electrodeposition. *J. Alloys Compd.* 762, 115-124. https://doi.org/10.1016/j.jallcom.2018.05.097.

Kayali, Y., Talaş, Ş. (2019). Investigation of wear and corrosion behaviour of AISI 316 L stainless steel coated by ESD surface modification. *Prot. Met. Phys. Chem. Surf.* 55, 1148-1153. https://doi.org/10.1134/S2070205119060170.

Kayali, Y., Talaş, Ş. (2021). Investigation on Wear Behavior of Steels Coated with WC by ESD Technique. *Prot. Met. Phys. Chem. Surf.* 57, 106-112. https://doi.org/10.1134/S2070205120060131.

Kim, Y.J., Shin, H., Park, H., Lim, J.D. (2008). Investigation into mechanical properties of austempered ductile cast iron (ADI) in accordance with austempering temperature. *Mater. Lett.* 62 (3), 357-360. https://doi.org/10.1016/j.matlet.2007.05.028.

Korkmaz, K. (2015). Investigation and characterization of electrospark deposited chromium carbide-based coating on the steel. *Surf. Coat. Tech.* 272, 1-7. https://doi.org/10.1016/j.surfcoat.2015.04.033.

Ling, C.L., Yajid, M.A.M., Tamin, M.N., Kamarudin, M., Taib, M.A.A., Nosbi, N., Ali, W.F.F.W. (2022). Effect of substrate roughness and PVD deposition temperatures on hardness and wear performance of AlCrN-coated WC-Co. *Surf. Coat. Tech.* 436, 128304. https://doi.org/10.1016/j.surfcoat.2022.128304.

Luo, H., Leitch, M., Behnamian, Y., Ma, Y., Zeng, H., Luo, J.L. (2015). Development of electroless Ni–P/nano-WC composite coatings and investigation on its properties. *Surf. Coat. Tech.* 277, 99-106. https://doi.org/10.1016/j.surfcoat.2015.07.011.

Méndez-Medrano, K.O., Martínez-González, C.J., Alvarado-Hernández, F., Jiménez, O., Baltazar-Hernández, V.H., Ruiz-Luna, H. (2018). Microstructure and Properties Characterization of WC-Co-Cr Thermal Spray Coatings. *JMMCE* 6 (4), 482-497. https://doi.org/10.4236/jmmce.2018.64034.

Moormann, R. (2011). Phenomenology of Graphite Burning in Air Ingress Accidents of HTRs. *Sci. Technol. Nucl. Install.,* Article ID 589747, https://doi:10.1155/2011/589747.

Moura e Silva, C.W., Branco, J.R.T., Cavaleiro, A. (2006). Characterization of magnetron co-sputtered W-doped C-based films. *Thin Solid Films* 515 (3), 1063-1068. https://doi.org/10.1016/j.tsf.2006.07.084.

Pagano, N., Angelini, V., Ceschini, L., Campana, G. (2016). Laser Remelting for Enhancing Tribological Performances of a Ductile Iron. *Procedia CIRP* 41, 987-991, https://doi.org/10.1016/j.procir.2015.12.131.

Phan, H.T., Tieu, A.K., Zhu, H., Kosasih, B., Zhu, Q., Grima, A., Ta, T.D. (2017). A study of abrasive wear on high-speed steel surface in hot rolling by Discrete Element Method. *Tribol. Int.* 110, 66-76. https://doi.org/10.1016/j.triboint.2017.01.034.

Rezende, B.A., dos Santos, A.J., Câmara, M.A., do Carmo, D.J., Houmard, M., Rodrigues, A.R., Campos Rubio, J.C. (2019). Characterization of ceramics coatings processed by Sol-Gel for cutting tools. *Coatings* 9 (11), 755. https://doi.org/10.3390/coatings9110755.

Ruijun, W., Yiyu, Q., Jun, L. (2005). Interface behavior study of WC92–Co8 coating produced by electrospark deposition. *Appl. Surf. Sci.* 240 (1-4), 42-47. https://doi.org/10.1016/j.apsusc.2004.05.299.

Rukanskis, M. (2019). Control of metal surface mechanical and tribological characteristics using cost effective electro-spark deposition. *Surf. Eng. Appl. Electrochem.* 55, 607-619. https://doi.org/10.3103/S1068375519050107.

Tieu, A.K., Zhu, Q., Zhu, H., Lu, C. (2011). An investigation into the tribological behaviour of a work roll material at high temperature. *Wear* 273 (1), 43-48. https://doi.org/10.1016/j.wear.2011.06.003.

Vernhes, L., Azzi, M., Klemberg-Sapieha, J.E. (2013). Alternatives for hard chromium plating: Nanostructured coatings for severe-service valves. *Mater. Chem. Phys.* 140 (2-3), 522-528. https://doi.org/10.1016/j.matchemphys.2013.03.065.

Wang, J.S., Meng, H.M., Yu, H.Y., Fan, Z.S., Sun, D.B. (2009). Characterization and wear behavior of WC-0.8 Co coating on cast steel rolls by electro-spark deposition. *Int. J. Miner. Metall. Mater.* 16 (6), 707-713. https://doi.org/10.1016/S1674-4799(10)60017-9.

Xu, L., Fan, X., Wei, S., Liu, D., Zhou, H., Zhang, G., Zhou, Y. (2017). Microstructure and wear properties of high-speed steel with high molybdenum content under rolling-sliding wear. *Tribol. Int.* 116, 39-46. https://doi.org/10.1016/j.triboint.2017.07.002.

Yang, Z.R., Li, D.S., Wang, L., Wang, S.Q., Wei, M.X. (2013). Wear behavior and mechanism of spheroidal graphite cast iron. *J. Iron Steel Res. Int.* 20 (10), 81-86. https://doi.org/10.1016/S1006-706X(13)60181-8.

Yuan, Z., Liu, L., Song, H., Lu, Z., Yang, B., Xiong, J., Jiang, X. (2021). Improvement in the universality of high-performance CVD diamond coatings on different WC-Co substrates by introducing multilayered diamond/Ş-SiC composite. *Diam. Relat. Mater.* 116, 108369. https://doi.org/10.1016/j.diamond.2021.108369.

Zhang, J., Zhang, N., Zhang, M., Lu, L., Zeng, D., Song, Q. (2014). Microstructure and mechanical properties of austempered ductile iron with different strength grades. *Mater. Lett.* 119, 47-50. https://doi.org/10.1016/j.matlet.2013.12.086.

Zhu, Y.C., Ding, C.X., Yukimura, K., Xiao, T.D., Strutt, P.R. (2001). Deposition and characterization of nanostructured WC–Co coating. *Ceram. Int.* 27 (6), 669-674. https://doi.org/10.1016/S0272-8842(01)00016-5.